How to cite: *Angew. Chem. Int. Ed.* **2022,** *61,* e202209099
International Edition: doi.org/10.1002/anie.202209099
German Edition: doi.org/10.1002/ange.202209099

Organic Synthesis

Regio- and Stereoselective 1,2-Oxyhalogenation of Non-Conjugated Alkynes via Directed Nucleopalladation: Catalytic Access to Tetrasubstituted Alkenes**

Mingyu Liu, Juntao Sun[+], Tao Zhang[+], Yi Ding, Ye-Qiang Han, Raúl Martín-Montero, Yu Lan, Bing-Feng Shi,* and Keary M. Engle**

Abstract: A catalytic 1,2-oxyhalogenation method that converts non-conjugated internal alkynes into tetrasubstituted alkenes with high regio- and stereoselectivity is described. Mechanistically, the reaction involves a Pd^{II}/Pd^{IV} catalytic cycle that begins with a directed oxypalladation step. The origin of regioselectivity is the preference for formation of a six-membered palladacycle intermediate, which is facilitated by an N,N-bidentate 2-(pyridin-2-yl)isopropyl (PIP) amide directing group. Selectivity for C(alkenyl)–X versus –N (X = halide) reductive elimination from the Pd^{IV} center depends on the identity of the halide anion; bromide and iodide engage in C(alkenyl)–X formation, while intramolecular C(alkenyl)–N reductive elimination occurs with chloride to furnish a lactam product. DFT calculations shed light on the origins of this phenomenon.

Introduction

Alkenes play a prominent role in organic chemistry due to their prevalence in functionally important molecules and their diverse chemical reactivity. The synthesis of highly substituted alkenes, especially those bearing tetrasubstitution, remains a major challenge due to both reactivity and selectivity issues. 1,2-Difunctionalization of internal alkynes represents a direct and efficient method to access tetrasubstituted alkenes.[1] However, the majority of traditional alkyne difunctionalization reactions are limited to conjugated alkynes or terminal alkynes.[1,2] Conjugated alkynes possess a polarized π-cloud that enhances reactivity and differentiates the two regioisomeric transition states in addition processes. In contrast, commonly encountered non-conjugated internal alkynes remain largely unexplored in 1,2-difunctionalizations.

Multicomponent, catalytic carbon-carbon π-bond functionalization reactions have recently attracted attention as empowering tools in organic synthesis.[3] In palladium(II)-catalyzed alkene functionalization, bidentate directing auxiliaries have enabled rapid discovery and development of a variety of historically challenging hydrofunctionalization and 1,2-difunctionalization reactions (Scheme 1A, top).[4] In these systems, the directing auxiliary recruits the Pd^{II} catalyst into close proximity to the alkene, resulting in π-Lewis acid activation, which facilitates regioselective *anti*-nucleopalladation or *syn*-migratory insertion.

Following an analogous blueprint, regio- and *E/Z*-stereoselective hydrofunctionalization of alkynes has been described.[5] However, extension to alkyne 1,2-difunctionalization has proven elusive to date (Scheme 1A, bottom). During our research, we have found that the conditions for directed, catalytic 1,2-difunctionalization of alkenes generally do not translate to analogous alkyne substrates and typically only afford a combination of unreacted alkyne starting material, hydrofunctionalization byproducts, or intractable reaction mixtures that stem from competitive processes (e.g., oligomerization). These observations underscore the difficulty of developing three-component 1,2-difunctionalizations of unactivated internal alkynes and speak to the unique geometry and reactivity of alkenyl palladacycles compared to their alkyl counterparts.[6,7] We expected careful tailoring of the directing auxiliary and

[*] M. Liu, J. Sun,[+] R. Martín-Montero, Prof. K. M. Engle
Department of Chemistry, The Scripps Research Institute
10550 N. Torrey Pines Road, La Jolla, CA 92037 (USA)
E-mail: keary@scripps.edu
T. Zhang,[+] Prof. Y. Lan
Green Catalysis Center and College of Chemistry,
Zhengzhou University
Zhengzhou, Henan, 450001 (P. R. China)
Y. Ding, Y.-Q. Han, Prof. B.-F. Shi
Department of Chemistry, Zhejiang University
Hangzhou, Zhejiang, 310027 (P. R. China)
E-mail: bfshi@zju.edu.cn
Prof. Y. Lan
School of Chemistry and Chemical Engineering, Chongqing Key Laboratory of Theoretical and Computational Chemistry,
Chongqing University
Chongqing, 400030 (P. R. China)
E-mail: lanyu@cqu.edu.cn
[+] The authors contributed equally to this work.

[**] A previous version of this manuscript has been deposited on a preprint server (https://doi.org/10.26434/chemrxiv-2022-kd15t).

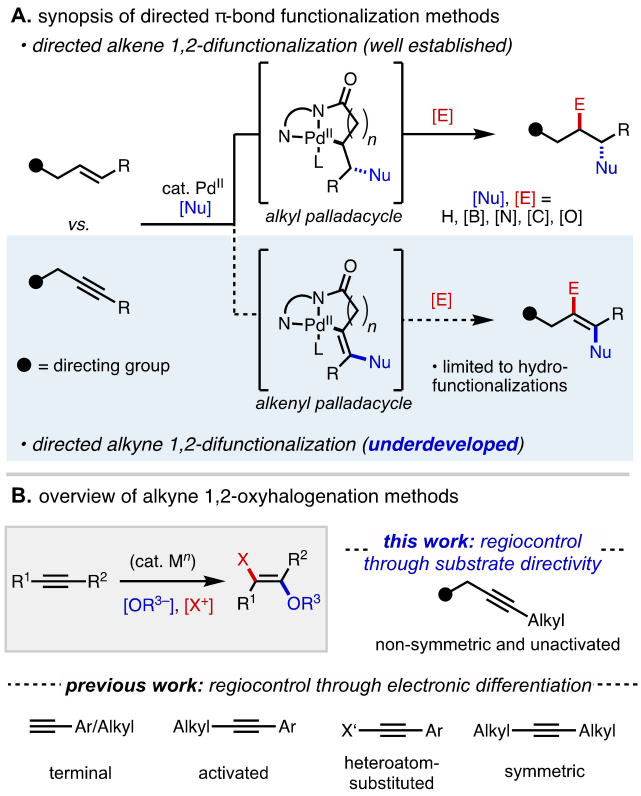

Scheme 1. Approaches to Directed Alkene/Alkyne Functionalization Reactions.

tuning of the redox potentials of the reagents employed would be required to surmount these challenges. Taking inspiration from recent reports in palladium-catalyzed C-(alkenyl)–H activation that invoke oxidative functionalization of C(alkenyl)–Pd intermediates,[8] we report the 1,2-oxyhalogenation of non-conjugated alkynes via six-membered alkenyl palladacycle intermediates enabled by the bidentate 2-(pyridin-2-yl)isopropyl (PIP) amide auxiliary, which grants access to fully substituted halo-enol esters that can be diversified through cross-coupling.[9]

Results and Discussion

We focused our attention on three-component 1,2-oxyhalogenation of alkynes,[2] given that this family of transformations can expediently assembly versatile and diversifiable substituted alkenes in a single operation (Scheme 1B). Existing methods, however, rely on electronic control of regioselectivity, limiting substrate scope to specific alkyne substitution patterns (Scheme 1B). We hypothesized that under Pd^{II}/Pd^{IV} catalysis, an alkyne bearing a suitable directing group could selectively react with a carboxylate nucleophile[10] and a halogen electrophile (Table 1).[11] After extensive screening, we identified effective reaction conditions using a combination of PivOH, TBAI, and PhI-$(OPiv)_2$ as coupling partners, $Pd(PhCN)_2Cl_2$ as catalyst, and MeCN as solvent at room temperature (entry 1). Under

Table 1: Optimization of conditions.

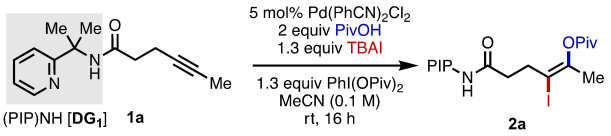

entry	variation from standard conditions	yield[a,b]
1	(none)	(87%)
2	AQ [DG_2]	58%
3	DG_3	56%
4	DG_4	49%
5	DG_5	65%
6	DG_6	n.d.
7	DG_7	n.d.
8	DG_8	trace
9	DG_9	trace
10	Oxone	n.d.
11	$K_2S_2O_8$	n.d.
12	Selectfluor	n.d.
13	$PhI(OTFA)_2$	n.d.

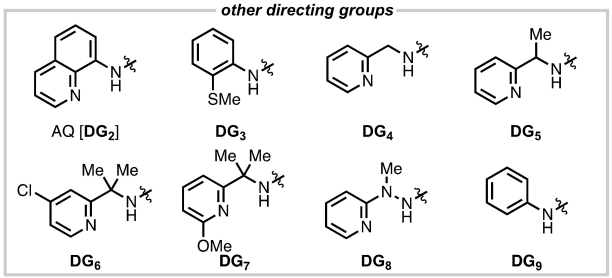

[a] ^{1}H NMR yield with CH_2Br_2 as internal standard. Isolated yield in parentheses. n.d. = not detected. [b] Reaction conditions: alkyne (0.05 mmol), PivOH (2 equiv), TBAI (1.3 equiv), $PhI(OPiv)_2$ (1.3 equiv), $Pd(PhCN)_2Cl_2$ (5 mol%), MeCN (0.1 M), r.t. = room temperature, 16 h.

these conditions, PIP-containing alkynyl amide **1a** underwent *anti*-1,2-oxyiodination to furnish **2a** in 87% yield. To summarize salient findings from optimization studies, we found that (PIP)NH outperformed other bidentate directing auxiliaries, including the 8-aminoquinoline-derived amide (AQ) that is widely used in alkene difunctionalization[4] and C(alkenyl)–H activation (entry 2).[8a] An N,S-bidentate directing group DG_3 was as effective as AQ but less effective than PIP(NH) (entry 3). The results with DG_4 and DG_5 illustrate the benefit of *gem*-substitution at the bridging carbon atom, possibly because enhanced steric hindrance and restricted conformational degrees of freedom promote C–I reductive elimination (entries 4 and 5).[12] Electronically tuned PIP amides (DG_6 and DG_7) were ineffective directing auxiliaries. Further experiments showed that an alternative N,N-bidentate structure, 1-methylhydrozinopyridine (DG_8), and a monodentate amide control (DG_9) did not facilitate the desired transformation (entries 6–9). Oxidants that have been previously reported in Pd^{II}/Pd^{IV} catalysis were ineffective (entries 10–13), demonstrating the unique properties of

carboxylate-containing hypervalent iodine reagent in this transformation.

We examined the substrate scope with a series of 4-pentynoic-acid-derived amides (Table 2). Alkynes with primary alkyl substituents offered good to high yields of the corresponding *E*-configured alkene products (**2a**–**2j**), consistent with an *anti*-nucleopalladation mechanism via an *exo*-alkenyl-palladacycle. The reaction could be conveniently performed on gram scale (**2a**, 2.5 mmol scale, 89 % yield). In addition, heteroatom-containing functional groups were compatible in the transformation (**2f**–**2j**), as was a cyclopropyl group (**2k**). Branched substrates containing substituents at the α (**2l**) or β (**2m**) position were lower-yielding, particularly in the latter case, which we attribute to sensitivity of the catalyst to steric hindrance proximal to the site of C–I bond formation.

We found that the stereochemical course of the reaction was influenced by the steric properties of the distal substituent on the alkyne. Sterically small (A-value <1.8) primary alkyl groups and (**2a**–**2j**) and a secondary cyclopropyl (**2k**) group reacted in an *anti*-fashion.[13] Cyclohexyl substitution (**2n**) (A-value $=2.2$) resulted in a 1.6:1 *E/Z* product mixture, reflecting the intermediate size of typical secondary alkyl groups. Sterically bulkier (A-value >2.8) tertiary alkyl groups resulted in highly selective *syn*-addition products (**2o**, **2p**). Aryl-substituted substrates also reacted in a *syn* fashion (**2q**, **2r**), though in this case electronic factors may also be at play. The stereochemistry of compound **2p** was determined by X-ray crystallography, and other compounds were assigned based on NMR spectroscopy (see Supporting Information).[14]

Beyond acid-derived amides, this method can be extended to 4-pentyn-1-amine derivatives masked with picolinamide-type directing groups (Table 2, **6a**–**6c**).[5] A methoxy-substituted directing group offered the highest yield in this case. Substrates with other tether lengths between the alkyne and the amide directing group that would react via a five- or seven-membered palladacycle did not yield appreciable oxyiodinated product under the standard conditions (see Figure S2 in the Supporting Information), illustrating the distance dependence of this catalytic system.

Different carboxylate nucleophiles were also tested and afforded products in good to excellent yields (Scheme 2, **2r**–**2t**). To avoid carboxylate scrambling, hypervalent iodide reagents pre-loaded with the desired carboxylate nucleophile were used. These reagents can be prepared by simply exchanging the ligand of the commercially available (diacetoxyiodo)benzene with the corresponding carboxylic acid. Other oxygen nucleophiles, including *t*-BuOH, PhOH, TFE, and HFIP, were examined but did not yield the desired product (see Figure S1 in the Supporting Information). Beyond 1,2-oxyiodination, we explored other halogen sources. As expected, 1,2-oxybromination (**2u**) was achieved with tetrabutylammonium bromide (TBAB). In contrast, with tetrabutylammonium chloride (TBAC), rather than the anticipated 1,2-oxychlorinated product, lactam **2v** was generated (see below for a mechanistic discussion of this point).[15,16]

Table 2: Substrate scope.

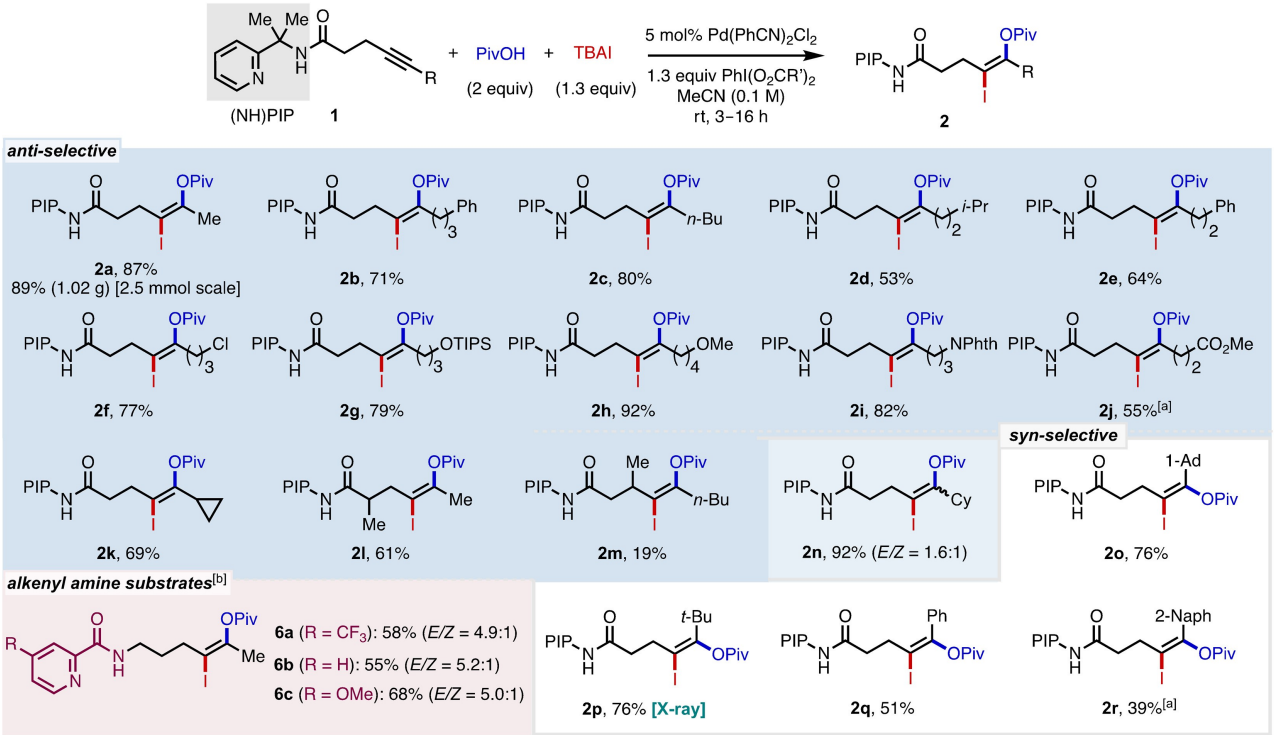

[a] 0.05 mmol scale. [b] $Pd(PhCN)_2Cl_2$ (10 mol%), 80 °C, 2 h.

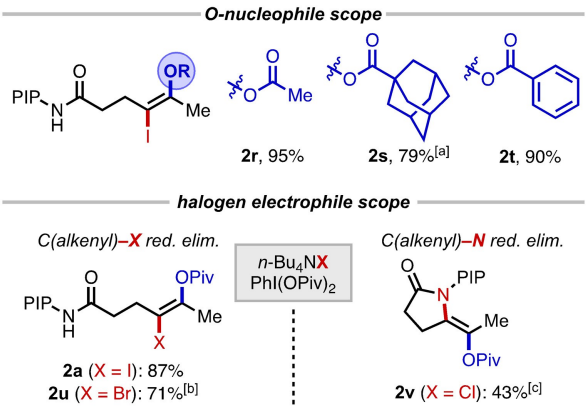

Scheme 2. Scope of nucleophile and electrophile. [a] 90 °C, 30 min. [b] 1,4-dioxane. [c] $Pd(MeCN)_2(OTs)_2$ (10 mol%).

The presence of the C(alkenyl)–I bond in the product offers a versatile handle for subsequent derivatization into diverse stereodefined tri- and tetrasubstituted alkenes. We thus examined several downstream transformations of the product with or without the PIP group attached (Scheme 3). First, with PIP-containing product **2a**, Sonogashira coupling generated enyne (**3b**), and Stille coupling resulted in styrenyl pivalate (**3c**). Alternatively, the C–I bond in **2a** could be reduced to a C–H bond via Pd-catalyzed hydrodehalogenation (**3d**). Removal of the PIP amide directing group proceeded upon treatment of **2a** with $NOBF_4$ to furnish the corresponding free carboxylic acid.[17] This intermediate was then converted to benzyl ester **3a** for the ease of manipulation. Additional synthetic transformations, including cyanation (**3e**), arylation (**3f**), and borylation (**3g**), furnished tetrasubstituted alkenes with unique substitution patterns.

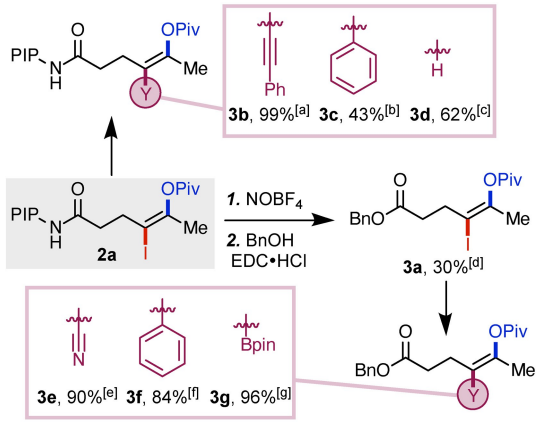

Scheme 3. Product transformations. [a] Reaction conditions: phenylacetylene (1.5 equiv), $Pd(OAc)_2$ (5 mol%), CuI (5 mol%), PPh_3 (10 mol%), Et_3N (0.4 M), 50 °C, 99% yield. [b] Reaction conditions: $PhSnBu_3$ (2.2 equiv), $Pd(PPh_3)_4$ (10 mol%), DMF (0.1 M), 80 °C, N_2, 43% yield. [c] Reaction conditions: HCO_2H (2.0 equiv), $Pd(OAc)_2$ (10 mol%), PPh_3 (20 mol%), Et_3N (3 equiv), DMF (0.1 M), 60 °C, 62% yield. [d] Reaction conditions: step 1) $NOBF_4$ (10 equiv), pyridine (0.05 M), −30 °C to 0 °C, 3 M HCl (aq.) work-up; step 2) BnOH (1.7 equiv), EDC·HCl (1.2 equiv), DMAP (10 mol%), DCM (0.15 M), r.t., 30% yield (over two steps). [e] Reaction conditions: $Zn(CN)_2$ (1.5 equiv), $Pd(PPh_3)_4$ (10 mol%), DMF (0.33 M), 80 °C, Ar, 90% yield. [f] Reaction conditions: $PhB(OH)_2$ (1.5 equiv), $Pd(PPh_3)_4$ (10 mol%), Cs_2CO_3 (3.0 equiv), THF (0.25 M), 90 °C, Ar, 84% yield. [g] Reaction conditions B_2pin_2 (2.0 equiv), $Pd(PPh_3)_4$ (10 mol%), Cs_2CO_3 (2.0 equiv), DCE (0.13 M), 80 °C, Ar, 96% yield. See Supporting Information for additional experimental details.

The high regio- and stereoselectivity of this catalytic reaction and the importance of the PIP directing group motivated us to examine its mechanism. Two general reaction paradigms could be envisioned. Following directed pivaloxypalladation, the alkenyl palladacycle could react directly with the oxidant (Scheme 4A, Path A). Alternatively, after pivaloxypalladation, reversible protodepalladation[5a,b,10] could give enol ester intermediate **3d** (Scheme 4A, Path B), which would then undergo C(alkenyl)–H activation[8b] to converge with the steps of Path A.

To distinguish between these possibilities, we performed a series of mechanistic studies. First, a control experiment under otherwise standard conditions without oxidant and TBAI did not result in conversion of **1a** to **3d** (Scheme 4B).[10,18] Second, in a trial under standard 1,2-oxyiodination conditions halted before full conversion, potential intermediate **3d** could not be detected (Scheme 4C). Along the same lines, when monitoring a standard 1,2-oxyiodination reaction by in situ ^1H NMR, **3d** could not be observed at any point during the course of the reaction (see Supporting Information).

These results establish that enol ester **3d** does not build up in detectable quantities during the reaction, but they do not fully exclude the possibility that **3d** is formed in small amounts but reacts much faster with the Pd^{II} catalyst than **1a**. Hence to probe the viability of Path B further,

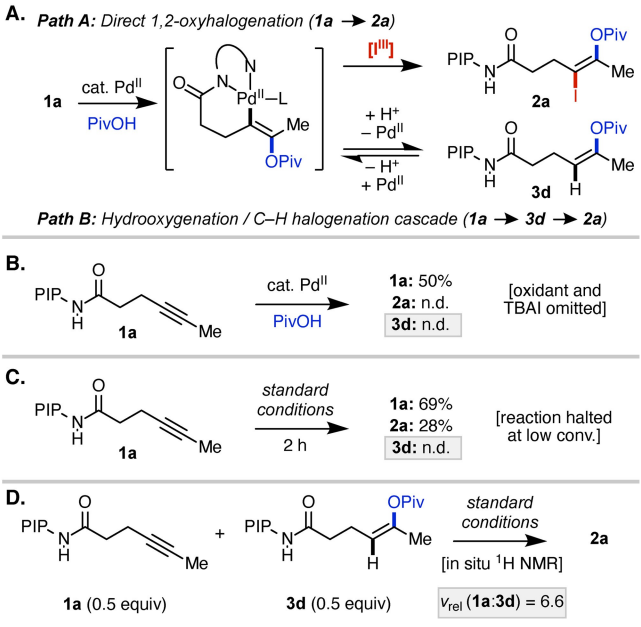

Scheme 4. Plausible reaction pathways and mechanistic studies.

independently synthesized **3d** (see Scheme 3) was subjected to the standard 1,2-oxyiodination conditions, and it was found that **3d** could indeed be converted to **2a** (Scheme S19C), establishing that **3d** is a competent intermediate. To gain insight into the *kinetic* competence of **3d**, we determined relative reactivities of **1a** and **3d** through a competition experiment between equimolar quantities of **1a** and **3d** under the standard reaction conditions (Scheme 4D). Alkyne **1a** reacts with an initial rate that is approximately 6.6 times faster than enol ester **3d**, and the rate of **3d** consumption accelerates as **1a** is consumed. This data is inconsistent with the scenario in which **3d** is formed in small quantities but is consumed much more rapidly that **1a**, supporting the direct difunctionalization as the predominant pathway (Scheme 4A, Path A).

The divergent stereochemical outcomes of the reaction with primary (**1a**–**1j**), secondary (**2k**, **2n**), and tertiary alkyl (**2o**, **2p**) of varying sizes were next considered. Two possible explanations for this data are (1) an initial stereoselective oxyiodination process followed by a secondary *E*/*Z* isomerization process[19] or (2) an oxyiodination process in which stereoselectivity is determined on-cycle in the nucleopalladation, oxidative addition, or reductive elimination steps. The first possibility was ruled out by preparing stereochemically pure samples of (*E*)-**2n** and (*Z*)-**2n**, which were generated as a separable 1.6:1 mixture from the catalytic oxyiodination reaction (Table 2). Subjecting each of these compounds to the standard reaction conditions did not lead to *E*/*Z* isomerization (Scheme 5), ruling out the first possibility and establishing that the *E*/*Z* stereochemistry is determined on-cycle. Further efforts to determine which step is stereochemical-determining by DFT were inconclusive.

Finally, to probe the origins of pathway selectivity for alkenyl halide versus lactam product formation, we turned to DFT calculations. As discussed above, nucleopalladation of the alkyne is proposed to generate an alkenyl palladacycle. Oxidation of the metal from Pd^{II} to Pd^{IV} then sets up a competition between C–X and C–N reductive elimination, which we speculated would be heavily influenced by the identity of the halide.

DFT calculations were performed with the M06 density functional, and several possible reaction pathways were considered for each of the counterions used in this study (X = I, Br, and Cl; for full energy profiles, see Supporting Information). The DFT results indicate that reductive elimination is the product-determining step, with one of two distinct pathways being preferred depending on the nature of the halide (Table 3). In the neutral pathway, which is favored with iodide and chloride, C–X (**TS-5-X**) or C–N reductive elimination (**TS-6-X**) takes place from a six-coordinate, κ^2-pivalate-bound neural Pd^{IV} center. In the anionic pathway, which is preferred for bromide, C–X (**TS-5b-X**) or C–N (**TS-6b-X**) reductive elimination takes place from an tri-halo, anionic Pd^{IV} ate species. The relative stabilities of the neutral versus anionic pathways largely reflect binding enthalpies of coordinating multiple halides for each of the different anions considered.[20] Consistent with experiment, C–I and C–Br bond formation are favored with respect to C–N bond formation by $\Delta\Delta G^{\ddagger} = 3.1$ kcal mol^{-1} and 4.3 kcal mol^{-1}, respectively. In contrast, C–N is favored compared to C–Cl bond formation by $\Delta\Delta G^{\ddagger} = 10.8$ kcal mol^{-1}.[21] We attribute the favorable nature of C–N reductive elimination in the case of X = Cl compared to the others to the decreasing Pd^{II}–X bond strength through the chloride, bromide, and iodide series,[22] as well as the decreased polarizability and higher electronegativity of chloride compared with the other halides examined.

Table 3: Summary of the lowest energy barriers of the reductive elimination pathways with different halides.

A. summary of halide effects

Entry	X =	preferred pathway	$\Delta G^{\ddagger}_{C-X\ RE}$ (kcal/mol)	$\Delta G^{\ddagger}_{C-N\ RE}$ (kcal/mol)
1	I	neutral	**8.1**	11.2
2	Br	anionic	**20.2**	24.5
3	Cl	neutral	19.2	**8.4**

B. reductive elimination transition states (neutral pathway)

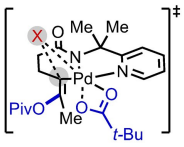

TS-5-X (C–X formation)

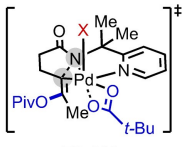

TS-6-X (C–N formation)

C. reductive elimination transition states (anionic pathway)

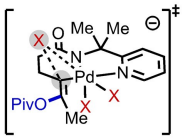

TS-5b-X (C–X formation)

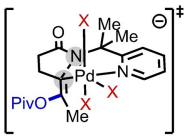

TS-6b-X (C–N formation)

Conclusion

In conclusion, we have developed a catalytic directed alkyne difunctionalization method to synthesize tetrasubstituted alkenes that proceeds with high regio- and stereoselectivity. A broad array of alkenyl amides, halides, and carboxylic acids are compatible in this reaction. The transformation can be performed on gram scale, and the amide auxiliary can be easily removed. Methods for downstream transformations have been developed to make structurally diverse tetrasubstituted alkenes. Experimental and computational studies shed light on the reaction mechanism and the

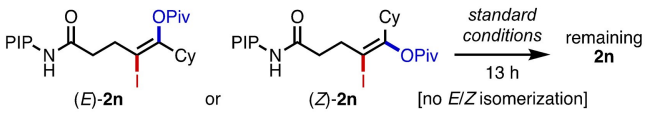

Scheme 5. Control experiments rule out the involvement of a secondary *E*/*Z*-isomerization process.

role of the halide anion in dictating pathway selectivity in the C–X versus C–N reductive elimination step from the Pd^{IV} center. We anticipate that this method and the underlying mechanistic insights will advance the development of synthetically enabling alkyne difunctionalization methods and expand the alkene synthesis toolkit.

Acknowledgements

This work was financially supported by the U.S. National Institutes of Health (R35GM125052) and the National Science Foundation of China (21925109 and 21822303). We gratefully acknowledge the Nankai University College of Chemistry for an International Research Scholarship (J.S.) and the La Caixa Foundation for a predoctoral fellowship (R.M.M.). Y. L. acknowledges support from the program for Science Technology Innovation Talents in Universities of Henan Province (No. 20HASTIT004). We thank Prof. Arnold L. Rheingold and Dr. Milan Gembicky (UCSD) for X-ray crystallographic analysis. We are grateful to Dr. Jason S. Chen, Brittany Sanchez, and Emily Sturgell for assistance with prep-LC purification and HRMS analysis. We thank Dr. Yingyu Liu and Camille Z. Rubel for detailed proofreading of this manuscript.

Conflict of Interest

The authors declare no conflict of interest.

Data Availability Statement

The data that support the findings of this study are openly available in CCDC at http://www.ccdc.cam.ac.uk/structures, reference number 2033977.

Keywords: Alkene · Alkyne Functionalization · Directing Group · Oxyhalogenation · Palladium

[1] a) B. M. Trost, C.-J Li, *Modern Alkyne Chemistry. Catalytic and Atom-Economic Transformations*, Wiley-VCH, Weinheim, **2015**; b) Y. Shimizu, M. Kanai, *Tetrahedron Lett.* **2014**, *55*, 3727–3737; c) T. Besset, T. Poisson, X. Pannecoucke, *Eur. J. Org. Chem.* **2015**, 2765–2789; d) Y. Yamamoto, I. D. Gridnev, N. T. Patil, T. Jin, *Chem. Commun.* **2009**, 5075–5087.

[2] For alkyne 1,2-iodooxygenation methods relevant to this study, see: a) Y. Ogata, I. Urasaki, *J. Org. Chem.* **1971**, *36*, 2164–2168; b) J. Barluenga, M. A. Rodriguez, P. J. Campos, *J. Org. Chem.* **1990**, *55*, 3104–3106; c) T. Kitamura, R. Furuki, H. Taniguchi, P. J. Stang, *Tetrahedron Lett.* **1990**, *31*, 703–704; d) T. Kitamura, R. Furuki, H. Taniguchi, P. J. Stang, *Tetrahedron* **1992**, *48*, 7149–7156; e) T. Muraki, H. Togo, M. Yokoyama, *J. Org. Chem.* **1999**, *64*, 2883–2889; f) Z. Chen, J. Li, H. Jiang, S. Zhu, Y. Li, C. Qi, *Org. Lett.* **2010**, *12*, 3262–3265; g) N. Okamoto, Y. Miwa, H. Minami, K. Takeda, R. Yanada, *J. Org. Chem.* **2011**, *76*, 9133–9138; h) X.-F. Xia, Z. Gu, W. Liu, N. Wang, H. Wang, Y. Xia, H. Gao, X. Liu, *Org. Biomol. Chem.* **2014**, *12*, 9909–9913; i) D. L. Priebbenow, R. W. Gable, J. Baell, *J. Org. Chem.* **2015**, *80*, 4412–4418; j) W. Ding, J. Chai, C. Wang, J. Wu, N. Yoshikai, *J. Am. Chem. Soc.* **2020**, *142*, 8619–8624.

[3] For recent reviews, see: a) G. Yin, X. Mu, G. Liu, *Acc. Chem. Res.* **2016**, *49*, 2413–2423; b) J. Derosa, V. T. Tran, V. A. van der Puyl, K. M. Engle, *Aldrichimica Acta* **2018**, *51*, 21–32; c) L. M. Wickham, R. Giri, *Acc. Chem. Res.* **2021**, *54*, 3415–3437; d) H.-Y. Tu, S. Zhu, F.-L. Qing, L. Chu, *Synthesis* **2020**, *52*, 1346–1356; e) A. Bahamonde, *Trends Chem.* **2021**, *3*, 863–876.

[4] For representative reports, see: a) J. A. Gurak Jr., K. S. Yang, Z. Liu, K. M. Engle, *J. Am. Chem. Soc.* **2016**, *138*, 5805–5808; b) K. S. Yang, J. A. Gurak Jr., Z. Liu, K. M. Engle, *J. Am. Chem. Soc.* **2016**, *138*, 14705–14712; c) Z. Liu, T. Zeng, K. S. Yang, K. M. Engle, *J. Am. Chem. Soc.* **2016**, *138*, 15122–15125; d) Z. Liu, Y. Wang, Z. Wang, T. Zeng, P. Liu, K. M. Engle, *J. Am. Chem. Soc.* **2017**, *139*, 11261–11270; e) R. Matsuura, T. C. Jankins, D. E. Hill, K. S. Yang, G. M. Gallego, S. Yang, M. He, F. Wang, R. P. Marsters, I. McAlpine, K. M. Engle, *Chem. Sci.* **2018**, *9*, 8363–8368; f) H. Wang, Z. Bai, T. Jiao, Z. Deng, H. Tong, G. He, Q. Peng, G. Chen, *J. Am. Chem. Soc.* **2018**, *140*, 3542–3546; g) H.-C. Shen, L. Zhang, S.-S. Chen, J. Feng, B.-W. Zhang, Y. Zhang, X. Zhang, Y.-D. Wu, L.-Z. Gong, *ACS Catal.* **2019**, *9*, 791–797; h) S. K. Nimmagadda, M. Liu, M. K. Karunananda, D.-W. Gao, O. Apolinar, J. S. Chen, P. Liu, K. M. Engle, *Angew. Chem. Int. Ed.* **2019**, *58*, 3923–3927; *Angew. Chem.* **2019**, *131*, 3963–3967; i) Z. Liu, X. Li, T. Zeng, K. M. Engle, *ACS Catal.* **2019**, *9*, 3260–3265; j) Z. Bai, S. Zheng, Z. Bai, F. Song, H. Wang, Q. Peng, G. Chen, G. He, *ACS Catal.* **2019**, *9*, 6502–6509; k) Y. Zhang, G. Chen, D. Zhao, *Chem. Sci.* **2019**, *10*, 7952–7957; l) Z. Bai, Z. Bai, F. Song, H. Wang, G. Chen, G. He, *ACS Catal.* **2020**, *10*, 933–940; m) H.-Q. Ni, I. Kevlishvili, P. G. Bedekar, J. S. Barber, S. Yang, M. Tran-Dubé, A. M. Romine, H.-X. Lu, I. McAlpine, P. Liu, K. M. Engle, *Nat. Commun.* **2020**, *11*, 6432; n) C.-F. Zhu, C.-H. Gao, W.-J. Hao, Y.-L. Zhu, S.-J. Tu, D.-C. Wang, B. Jiang, *Org. Chem. Front.* **2021**, *8*, 127–132; o) R. K. Shukla, A. K. Chaturvedi, S. Pal, C. M. R. Volla, *Org. Lett.* **2021**, *23*, 1440–1444; p) R. K. Shukla, A. K. Chaturvedi, C. M. R. Volla, *ACS Catal.* **2021**, *11*, 7750–7761; q) L. Xia, Y. Wu, C. Lin, F. Gao, L. Shen, *Asian J. Org. Chem.* **2022**, *11*, e202100742.

[5] a) Z. Liu, J. Derosa, K. M. Engle, *J. Am. Chem. Soc.* **2016**, *138*, 13076–13081; b) J. Derosa, A. L. Cantu, M. N. Boulous, M. L. O'Duill, J. L. Turnbull, Z. Liu, D. M. De La Torre, K. M. Engle, *J. Am. Chem. Soc.* **2017**, *139*, 5183–5193.

[6] M. Liu, J. Sun, K. M. Engle, *Tetrahedron* **2022**, *103*, 132513.

[7] a) J. He, M. Wasa, K. S. L. Chan, Q. Shao, J.-Q. Yu, *Chem. Rev.* **2017**, *117*, 8754–8786; b) A. S. Suseelan, A. Dutta, G. K. Lahiri, D. Maiti, *Trends Chem.* **2021**, *3*, 188–203; c) B. Liu, A. M. Romine, C. Z. Rubel, K. M. Engle, B.-F. Shi, *Chem. Rev.* **2021**, *121*, 14957–15074.

[8] a) M. Liu, P. Yang, M. K. Karunananda, Y. Wang, P. Liu, K. M. Engle, *J. Am. Chem. Soc.* **2018**, *140*, 5805–5813; b) B. S. Schreib, E. M. Carreira, *J. Am. Chem. Soc.* **2019**, *141*, 8758–8763; c) K. Meng, T. Li, C. Yu, C. Shen, J. Zhang, G. Zhong, *Nat. Commun.* **2019**, *10*, 5109; d) Z. Wu, N. Fatuzzo, G. Dong, *J. Am. Chem. Soc.* **2020**, *142*, 2715–2720; e) B. S. Schreib, M. Fadel, E. M. Carreira, *Angew. Chem. Int. Ed.* **2020**, *59*, 7818–7822; *Angew. Chem.* **2020**, *132*, 7892–7896.

[9] a) Q. Zhang, B.-F. Shi, *Chin. J. Chem.* **2019**, *37*, 647–656; b) Q. Zhang, B.-F. Shi, *Acc. Chem. Res.* **2021**, *54*, 2750–2763.

[10] a) N. Tsukada, A. Takahashi, Y. Inoue, *Tetrahedron Lett.* **2011**, *52*, 248–250; b) J. Corpas, E. M. Arpa, R. Lapierre, I. Corral, P. Mauleón, R. G. Arrayás, J. C. Carretero, *ACS Catal.* **2022**, *12*, 6596–6605.

[11] a) S. R. Whitfield, M. S. Sanford, *J. Am. Chem. Soc.* **2007**, *129*, 15142–15143; b) K. J. Stowers, M. S. Sanford, *Org. Lett.* **2009**, *11*, 4584–4587; c) D. C. Powers, T. Ritter, *Nat. Chem.* **2009**, *1*,

302–309; d) D. C. Powers, D. Benitez, E. Tkatchouk, W. A. Goddard III, T. Ritter, *J. Am. Chem. Soc.* **2010**, *132*, 14092–14103; e) T. Furuya, D. Benitez, E. Tkatchouk, A. E. Strom, P. Tang, W. A. Goddard III, T. Ritter, *J. Am. Chem. Soc.* **2010**, *132*, 3793–3807; f) X.-C. Wang, Y. Hu, S. Bonacorsi, Y. Hong, R. Burrell, J.-Q. Yu, *J. Am. Chem. Soc.* **2013**, *135*, 10326–10329; g) L. Chu, X.-C. Wang, C. E. Moore, A. L. Rheingold, J.-Q. Yu, *J. Am. Chem. Soc.* **2013**, *135*, 16344–16347; h) L. Chu, K.-J. Xiao, J.-Q. Yu, *Science* **2014**, *346*, 451–455; i) R.-Y. Zhu, T. G. Saint-Denis, Y. Shao, J. He, J. D. Sieber, C. H. Senanayake, J.-Q. Yu, *J. Am. Chem. Soc.* **2017**, *139*, 5724–5727; j) R.-Y. Zhu, L.-Y. Liu, J.-Q. Yu, *J. Am. Chem. Soc.* **2017**, *139*, 12394–12397; k) Q.-L. Yang, X.-Y. Wang, T.-L. Wang, X. Yang, D. Liu, X. Tong, X.-Y. Wu, T.-S. Mei, *Org. Lett.* **2019**, *21*, 2645–2649 For a review, see: l) G. Liao, B.-F. Shi, *Acta Chim. Sin.* **2015**, *73*, 1283–1293.

[12] a) M. E. Jung, G. Piizzi, *Chem. Rev.* **2005**, *105*, 1735–1766. For a buried volume comparison of AQ and PIP, see: b) Z. Liu, L. J. Oxtoby, Z. Q. Li, N. Kim, G. H. M. Davies, K. M. Engle, *ChemRxiv.* **2022**, https://doi.org/10.26434/chemrxiv-2022-t2zb4.

[13] E. V. Anslyn, D. A. Dougherty, *Modern Physical Organic Chemistry*, University Science Books, United States, **2006**, p. 104.

[14] Deposition number 2033977 (**2p**) contains the supplementary crystallographic data for this paper. These data are provided free of charge by the joint Cambridge Crystallographic Data Centre and Fachinformationszentrum Karlsruhe Access Structures service.

[15] For a related reaction, see: Y. Ding, Y.-Q. Han, L.-S. Wu, T. Zhou, Q.-J. Yao, Y.-L. Feng, Y. Li, K.-X. Kong, B.-F. Shi, *Angew. Chem. Int. Ed.* **2020**, *59*, 14060–14064; *Angew. Chem.* **2020**, *132*, 14164–14168.

[16] Varying only the TBAX salt under otherwise standard conditions from Table 2, **2u** and **2v** were obtained in 24 % and 30 % yield, respectively. A small amount of diacetoxylated byproduct was observed in the crude reaction mixture in the former case, whereas no byproducts were detected in the latter. Additional optimization led to the conditions shown in Scheme 2.

[17] D. Dailler, G. Danoun, O. A. Baudoin, *Angew. Chem. Int. Ed.* **2015**, *54*, 4919–4922; *Angew. Chem.* **2015**, *127*, 5001–5004.

[18] F. Alonso, I. P. Beletskaya, M. Yus, *Chem. Rev.* **2004**, *104*, 3079–3159.

[19] C. M. Le, P. J. C. Menzies, D. A. Petrone, M. Lautens, *Angew. Chem. Int. Ed.* **2015**, *54*, 254–257; *Angew. Chem.* **2015**, *127*, 256–259.

[20] With X = Br, an intermediate with three bromide ligands coordinated to the Pd^{IV} center is computed to be much more stable than the analogous intermediates with other halides, which is the reason for the higher transition state energies of 20.2 kcal mol^{-1} and 24 kcal mol^{-1} for C–Br and C–N reductive elimination.

[21] Two other pathways that would explain lactam formation in the case of chloride would be: (1) C–Cl reductive elimination, followed by azapalladation onto the resulting alkenyl chloride and finally β-Cl elimination; and (2) azapalladation of the PIP amide onto the alkyne, followed by Pd^{II}/Pd^{IV} oxidative addition and C-OPiv reductive elimination. While these pathways cannot be fully ruled out, they are viewed as less likely based on the available experimental and computational data.

[22] a) K. K. Pandey, P. Patidar, H. Braunschweig, *Inorg. Chem.* **2010**, *49*, 6994–7000; b) J. G. P. Delis, P. G. Aubel, K. Vrieze, P. W. N. M. van Leeuwen, N. Veldman, A. L. Spek, *Organometallics* **1997**, *16*, 4150–4160; c) B. P. Carrow, J. F. Hartwig, *J. Am. Chem. Soc.* **2011**, *133*, 2116–2119.

Manuscript received: June 21, 2022
Accepted manuscript online: September 8, 2022
Version of record online: September 29, 2022